Article

Not peer-reviewed version

The Effect of Sample Configuration on the Measurement of the Bending Properties of Extruded Polystyrene Using Three-Point, Four-Point, and Compression Bending Tests

Hiroshi Yoshihara * , Masahiro Yoshinobu , Makoto Maruta

Posted Date: 17 May 2024

doi: 10.20944/preprints202405.1113.v1

Keywords: extruded polystyrene; three-point bending test; four-point bending test; compression bending test; Young's modulus; proportional limit stress; bending strength

Article

The Effect of Sample Configuration on the Measurement of the Bending Properties of Extruded Polystyrene Using Three-Point, Four-Point, and Compression Bending Tests

Hiroshi Yoshihara [1,*], Masahiro Yoshinobu [2] and Makoto Maruta [3]

[1] Faculty of Science and Engineering, Shimane University, Nishikawazu-cho 1060, Matsue, Shimane 690-8504, Japan
[2] Faculty of Science and Engineering, Shimane University, Nishikawazu-cho 1060, Matsue, Shimane 690-8504, Japan; yosinobu@riko.shimane-u.ac.jp
[3] Faculty of Science and Technology, Shizuoka Institute of Science and Technology, Toyosawa 2200-2, Fukuroi, Shizuoka 437-8555, Japan; maruta.makoto@sist.ac.jp
* Correspondence: Correspondence: yosihara@riko.shimane-u.ac.jp; Tel.: +81-852-32-6508

Abstract: Extruded polystyrene (XPS) is frequently used in the construction of many different structures. It is therefore necessary to appropriately characterize its mechanical properties to ensure the safety of said structures. Among the available characterization tests, static bending tests are simple and easy to perform; owing to these characteristics, they should be performed more frequently than other tests. However, in static bending tests on XPS, there are several challenges owing to the high flexibility of XPS, and the chosen testing method and sample configuration affect the accuracy of characterization. In this study, three bending properties (Young's modulus, proportional limit stress, and bending strength) of samples cut from an XPS panel were determined using three-point bending (TPB), four-point bending (FPB), and compression bending (CB) tests with varying sample span/depth ratios, and statistical analyses were performed to determine the relevance of the tests. The experimental results suggest that the TPB and CB tests were more feasible than the FPB test when the span/depth ratio was appropriately determined. However, clear differences were observed in the sample bending properties determined in these tests. In light of these findings, further studies should be conducted to elucidate these differences.

Keywords: extruded polystyrene; three-point bending test; four-point bending test; compression bending test; Young's modulus; proportional limit stress; bending strength

1. Introduction

Extruded polystyrene (XPS) possesses excellent thermal insulation properties; owing to these properties, it is frequently used as an insulating heat source in many different structures [1–5]. Of late, XPS panels have been used for floorings [6–8] and as sandwich panels [9–12] because their lightweight nature attenuates seismic forces. Additionally, the exceptional processability of XPS enhances its structural utilization. Therefore, adequate characterization of the mechanical properties of XPS is necessary to ensure the safety of structure in which XPS is used as the structural element.

A number of mechanical tests have been utilized to characterize the mechanical properties of foam materials, including XPS, such as static compression [4,13–16], static tension [15], flexural vibration [16,17], static shear [13,17,18], torsional vibration [18], asymmetric four-point bending [18], and static bending tests [4,14–16]. Among these tests, the static bending test is simple and easy to perform; therefore, to characterize the mechanical properties of XPS, this particular test should be used more frequently. In addition, three-point bending (TPB) tests of cellular plastics are standardized in ISO 1209-2:2004 [19] and JIS K 7221-2:2006 [20]; therefore, these standards have resulted in the increased utilization of TPB test. In addition, the four-point bending (FPB) test is used as frequently as TPB tests. However, at present, there are a number of concerns regarding the

 doi:10.20944/preprints202405.1113.v1

measurement of the mechanical properties of XPS, such as the Young's modulus, proportional limit stress, and bending strength. When a sample is not sufficiently slender, the deflection induced by the shearing force affects the measurement of the Young's modulus and the proportional limit stress. In contrast, when a sample is extremely slender, the load–deflection behavior in the large deflection range deviates from that derived using elementary beam theory (EBT) because of the significant flexibility of XPS, and the bending strength cannot be predicted appropriately using equations based on EBT. Therefore, to appropriately characterize the bending properties of XPS using the aforementioned tests, the effect of the sample configuration must be considered in more detail. Independent of the TPB and FPB tests, compression bending (CB) tests have been performed using numerous carbon fiber-reinforced plastics (CFRP) [21–23]. In the CB test, bending deformation is induced by applying an axial load to the sample, and the load–deflection relationship can be determined based on elastica theory. Because the CB test can be performed without applying a lateral load to the sample body, there is no stress concentration due to the lateral load, and bending failure due to the stress concentration can be avoided. CB tests involving solid wood [24], plywood and medium-density fiberboard (MDF) [25,26], and cardboard samples [27] at various span/depth ratios have been performed in previous studies, and the bending properties of these samples could be determined appropriately while reducing the effect of the sample configuration in the relevant span/depth ratio range. If the CB test, as well as the TPB and FPB tests, is applicable to measure the bending properties of XPS, then this shows great promise in the field.

In this study, TPB, FPB, and CB tests were performed using XPS samples at various span/depth ratios. The effects of the chosen testing methods and sample configurations were examined through the use of analysis of variance (ANOVA), and the most feasible method for characterizing the bending properties of these samples was investigated using statistical analyses.

2. Theoretical Background

Figures 1a-c illustrate the diagrams of the TPB, FPB, and CB tests, respectively.

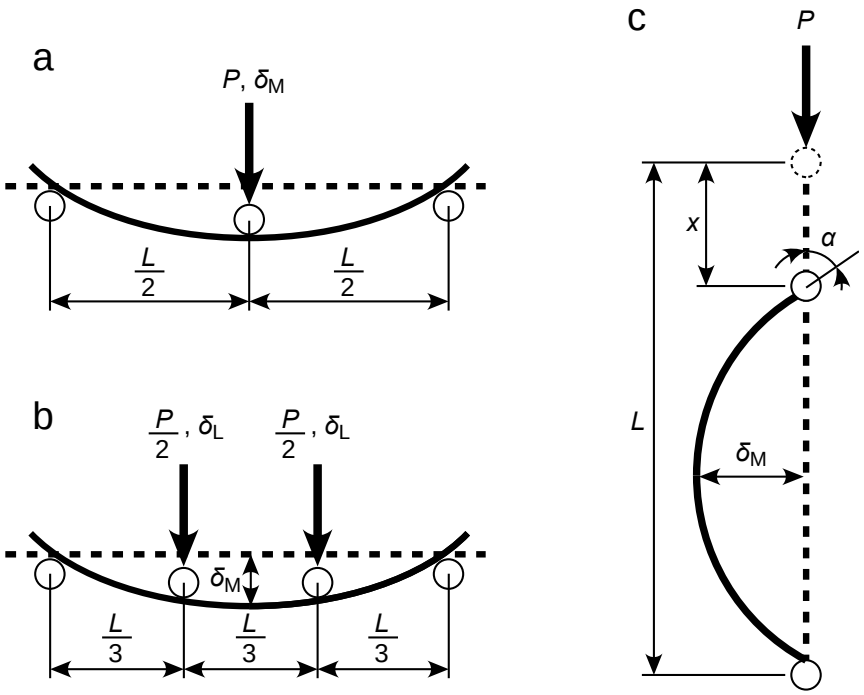

Figure 1. Diagrams of the TPB (a), FPB (b), and CB (c) tests.

The TPB test method is standardized by the International Organization for Standardization and Japanese Industrial Standards as ISO 1209-02:2004 [19] and JIS K 7221-2:2006 [20], respectively, for characterizing the bending properties of rigid cellular plastics. The load applied to the midspan P

 doi:10.20944/preprints202405.1113.v1

and deflection at midspan δ_M can be obtained, as shown in Figure 1a. From EBT, the Young's modulus in the length direction of the sample E_x is obtained as follows:

$$E_x = \frac{3L^3}{4BH^3} \cdot \frac{\Delta P}{\Delta \delta_M} \quad (1)$$

where L is the distance between the spans, B and H are the width and depth of the sample, respectively, and $\Delta P/\Delta\delta_M$ represents the slope of the straight line drawn along the initial linear segment in the P-δ_M relationship. The bending stress at the outer surface of the midspan σ_x is also derived from EBT as follows:

$$\sigma_x = \frac{3PL}{2BH^2} \quad (2)$$

Therefore, the proportional limit stress Y_x is determined as

$$Y_x = \frac{3P_{NL}L}{2BH^2} \quad (3)$$

where P_{NL} is the load where the aforementioned straight line deviates from the P-δ_M curve. The method used to determine P_{NL} values is described below. The bending strength F_x can be obtained by substituting the maximum load P_{max} into P in Eq. (2). However, when the deflection is extremely large, the direction of the reaction force from the supporting point is inclined rather than positioned upward; therefore, it is often difficult to determine the load–deflection relationship and bending strength using EBT. For carbon fiber reinforced plastics (CFRP), the methods used to calculate the bending strength are standardized with consideration of the effect of large deflection as ASTM D 790-17 [28] and JIS K 7074-1988 [29]. The equations determined in these standards were compared with those based on EBT as follows:

$$F_x = \begin{cases} \dfrac{3P_{max}L}{2BH^2} \text{ (EBT)} \\ \dfrac{3P_{max}L}{2BH^2}\left[1 + 6\left(\dfrac{\delta_{Mb}}{L}\right)^2 - 4\left(\dfrac{\delta_{Mb}}{L}\right)\left(\dfrac{H}{L}\right)\right] \text{ (ASTM D790 − 17)} \\ \dfrac{3P_{max}L}{2BH^2}\left[1 + 4\left(\dfrac{\delta_{Mb}}{L}\right)^2\right] \text{ (JIS K 7074 − 1988)} \end{cases} \quad (4)$$

where $\delta_{Mb} = \delta_M$ at $P = P_{max}$.

Although the FPB test used for rigid cellular plastics is not determined in major standards, it can be performed as easily as the TPB test; therefore, the FPB test methods for various materials have been determined by several major standards. As shown in Figure 1b, in the FPB test, two loads of $P/2$ are symmetrically applied to the trisectional points, and the deflection at the loading point is defined as δ_L. In the FPB test methods for CFRP standardized in ASTM D6272-17 [30] and JIS K 7074-1988 [31], the deflection is measured at the midspan using equipment such as a linear variable differential transformer (LVDT). However, for lightweight materials such as XPS, deflection cannot be measured accurately because the reaction force from the LVDT is often large, affecting the bending deformation of the sample. Instead of using an LVDT, δ_M is calculated from δ_L, based on EBT, as follows:

$$\delta_M = \frac{23}{20}\delta_L \quad (5)$$

Therefore, E_x and σ_x are obtained from EBT as follows:

$$E_x = \frac{23L^3}{108BH^3} \cdot \frac{\Delta P}{\Delta \delta_M} \quad (6)$$

and

$$\sigma_x = \frac{PL}{BH^2} \quad (7)$$

In the FPB test, Y_x is determined using Eq. (7) as:

 doi:10.20944/preprints202405.1113.v1

$$Y_x = \frac{P_{\mathrm{NL}} L}{B H^2} \tag{8}$$

In ASTM D 6272-17 [30] and JIS K 7074-1988 [31], the equations for FPB are also standardized, and they are demonstrated with the equation derived from EBT as:

$$F_x = \begin{cases} \dfrac{P_{\max} L}{B H^2} \ (\mathrm{EBT}) \\ \dfrac{P_{\max} L}{B H^2}\left[1 + 4.70\left(\dfrac{\delta_{\mathrm{Mb}}}{L}\right)^2 - 7.04\left(\dfrac{\delta_{\mathrm{Mb}}}{L}\right)\left(\dfrac{H}{L}\right)\right] \ (\mathrm{ASTM\ D6272-17}) \\ \dfrac{P_{\max} L}{B H^2}\left[1 + \dfrac{4644}{529}\left(\dfrac{\delta_{\mathrm{Mb}}}{L}\right)^2 - \dfrac{162}{23}\left(\dfrac{\delta_{\mathrm{Mb}}}{L}\right)\left(\dfrac{H}{L}\right)\right] \ (\mathrm{JIS\ K\ 7074-1988}) \end{cases} \tag{9}$$

In the CB test shown in Figure 1c, the angle between the vertical axis and length direction at the end of the sample is defined as α. In addition, the displacements at the loading point are defined as x, whereas the curvature at the midspan is defined as κ_{M}. According to elastica theory, x/L = 0-0.0676, 0.0676-0.259, and 0.259-0.543 in the ranges of α = 0-30°, 30-60°, and 60-90°, respectively, and the δ_{M}/L-x/L and $\kappa_{\mathrm{M}}L$-x/L relationships under the hinged ends are approximated as follows [27]:

$$\frac{\delta_{\mathrm{M}}}{L} = \begin{cases} 0.62390\left(\dfrac{x}{L}\right)^{0.49745} & (0 \le x/L \le 0.0676) \\ 0.54880\left(\dfrac{x}{L}\right)^{0.45036} & (0.0676 < x/L \le 0.259) \\ 0.47334\left(\dfrac{x}{L}\right)^{0.33983} & (0.259 < x/L \le 0.543) \end{cases} \tag{10}$$

and

$$\kappa_{\mathrm{M}} L = \begin{cases} 6.3625\left(\dfrac{x}{L}\right)^{0.50153} & (0 \le x/L \le 0.0676) \\ 6.8713\left(\dfrac{x}{L}\right)^{0.52978} & (0.0676 < x/L \le 0.259) \\ 7.5113\left(\dfrac{x}{L}\right)^{0.59634} & (0.259 < x/L \le 0.543) \end{cases} \tag{11}$$

From the relationships derived using Eq. (10), σ_x can be derived as

$$\sigma_x = \frac{6 P \delta_{\mathrm{M}}}{B H^2} \tag{12}$$

When the longitudinal strain at the midspan surface is defined as the bending strain ε_x, it is derived using κ_{M}, as follows:

$$\varepsilon_x = \frac{\kappa_{\mathrm{M}} H}{2} \tag{13}$$

E_x, Y_x, and F_x can be obtained using the σ_x-ε_x relationship derived from Eqs. (12) and (13).

2. Materials and Methods

2.1. Materials

The test samples used in this study were cut from an XPS panel (STYROFOAM B2; Dupont Styro Corporation, Tokyo, Japan) with initial dimensions of 1820, 910, and 25 mm in length, width, and thickness, respectively. The length, width, and thickness directions of the panel are defined as the L-, T-, and Z-axes, respectively. The panel was initially cut using a circular saw and finished to the final dimensions of the sample using a heat wire. The L-, T-, and Z-axes of the panel coincided with the length, depth, and width directions of the sample, respectively; therefore, sample width B was 25 mm. In contrast, the sample depths, H, were cut to 20 mm and 10 mm. For the sample with H = 20 mm, the length varied from 300 mm to 700 mm at intervals of 100 mm, incontrast, it varied from 550 mm to 700 mm at intervals of 50 mm for the sample with H = 10 mm. The distance between supports L varied from 100 to 500 mm at intervals of 100 mm and from 350 to 500 mm at intervals of 50 mm in

 doi:10.20944/preprints202405.1113.v1

the samples with H = 20 and 10 mm, respectively. Therefore, the L/H value was varied from 5 to 50 at intervals of 5. The sample was cut such that the length of the overhung portion was 100 mm. Five samples were used for each test. The density of the sample was 25.5 ± 0.3 kg/m^3.

2.2. TPB, FPB, and CB Tests

TPB, FPB, and CB tests were performed, and E_x, Y_x, and F_x values were obtained by varying the L/H value.

Figure 2 shows photographs of the TPB, FPB, and CB tests conducted in this study. In the TPB and FPB tests, as shown in Figures 2a and b, respectively, the sample was set on a pair of supports with a radius of 10 mm. A lateral load, P, was applied using a loading nose with a radius of 10 mm. In the CB test, when using a sample with H = 20 mm, cylindrical attachments were set on both ends of the sample to enhance bending deformation, and a load was applied via the cylindrical attachment using a steel plate, as shown in Figure 2c, to enhance the rotation at the sample ends. However, when using the sample with H = 10 mm, bending deformation was induced by the weight of the attachment set on the top of the sample prior to the application of the axial load, and E_x, Y_x, and F_x could not be appropriately determined using the σ_x-ε_x relationship. To solve this issue, the CB test was performed without the use of the top attachment, as shown in Figure 2d. Even under this condition, rotation was easily induced at the sample ends, and the bending properties were appropriately determined.

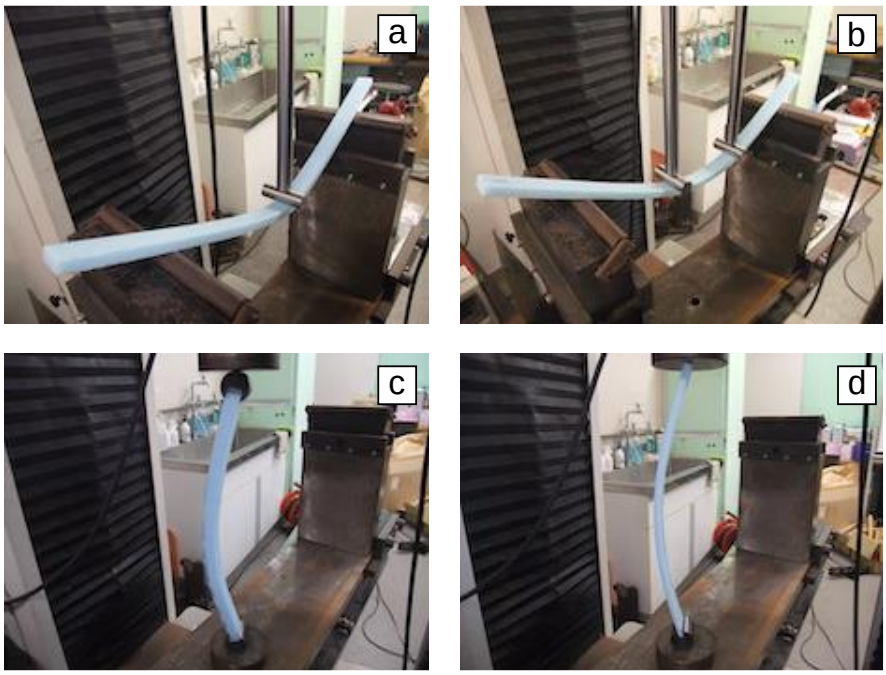

Figure 2. Photographs of the TPB test (a), FPB test (b), CB test using a sample with H = 20 mm (c), and CB test using a sample with H = 10 mm (d).

The crosshead speed $\dot{x}$ was derived from the following relationship [27,31]:

$$\dot{x} = \begin{cases} \dfrac{\dot{\varepsilon}_x L^2}{6H} \ (\text{TPB}) \\ \dfrac{23\dot{\varepsilon}_x L^2}{108H} \ (\text{FPB}) \\ L\left(\dfrac{0.31434\dot{\varepsilon}_x L}{H}\right)^{1.9939} \ (\text{CB}) \end{cases} \tag{14}$$

Similar to the results of a previous study, the strain rate at the midspan $\dot{\varepsilon}_x$ was determined to be 0.06 /sec [27]. Table 1 lists the crosshead speeds adopted under each test condition.

Table 1. Crosshead speed in the TPB, FPB, and CB tests.

 doi:10.20944/preprints202405.1113.v1

***H* (mm)**			**20**					**10**		
***L* (mm)**	**100**	**200**	**300**	**400**	**500**	**300**	**350**	**400**	**450**	**500**
L*/*H	**5**	**10**	**15**	**20**	**25**	**30**	**35**	**40**	**45**	**50**
TPB	5.0	20.0	45.0	80.0	125	90.0	123	160	203	250
FPB	6.39	25.6	57.5	102	160	115	156	205	259	319
CB	0.902	7.19	24.2	57.3	112	96.4	153	228	324	445

Unit of crosshead speed = mm/min.

As described above, the P-δ_M curve was obtained in the TPB and FPB tests, and $\Delta P/\Delta\delta_M$ and P_{NL} were determined from a straight line drawn along the initial linear segment of the P-δ_M curve. The P_{NL} value was determined using the load for deviation from linearity at half the thickness of the plotted curve [32]. E_x was determined by substituting $\Delta P/\Delta\delta_M$ into Eqs. (1) and (6) in the TPB and FPB tests, respectively. Additionally, Y_x was determined by substituting P_{NL} into Eqs. (3) and (8) for the TPB and FPB tests, respectively. In contrast, P_{max} was obtained from the maximum load, and F_x was determined by substituting P_{max} into Eqs. (4) and (9) for the TPB and FPB tests, respectively. The effects of the equations standardized in the ASTM and JIS standards were examined by comparing the results. In the CB test, E_x, Y_x, and F_x were directly determined from the σ_x-ε_x relationship obtained from Eqs. (12) and (13).

3. Results

In the TPB and FPB tests, the σ_x-ε_x relationship can be determined based on the results of EBT; therefore, the P-δ_M relationships were transformed into σ_x-ε_x relationships, and the effects of the test methods and sample configurations were compared using the σ_x-ε_x relationships. In the TPB, test, ε_x is derived as follows:

$$\varepsilon_x = \frac{6B\delta_M}{H^2} \tag{15}$$

In the FPB test, ε_x is derived as follows:

$$\varepsilon_x = \frac{108B\delta_M}{23H^2} \tag{16}$$

Figure 3 illustrates comparisons of the representative σ_x-ε_x relationships calculated using Eqs. (2) and (15) (TPB tests), Eqs. (7) and (16) (FPB tests), and Eqs. (12) and (13) (CB tests). In the TPB and FPB tests, when the L/H value is sufficiently low, bending failure is often induced in an unstable manner when σ_x reaches σ_{max}. In contrast, when the L/H value increases, this tendency is not enhanced; however, σ_x gradually decreases after it reaches σ_{max}. Additionally, the σ_{max} value obtained from EBT decreases as L/H increases, particularly in the FPB test results. In contrast, in the CB tests, the σ_x-ε_x relationships were found to be similar to one another, except for those with L/H values of 5 and 10, and bending failure was induced immediately after σ_x reaches σ_{max}.

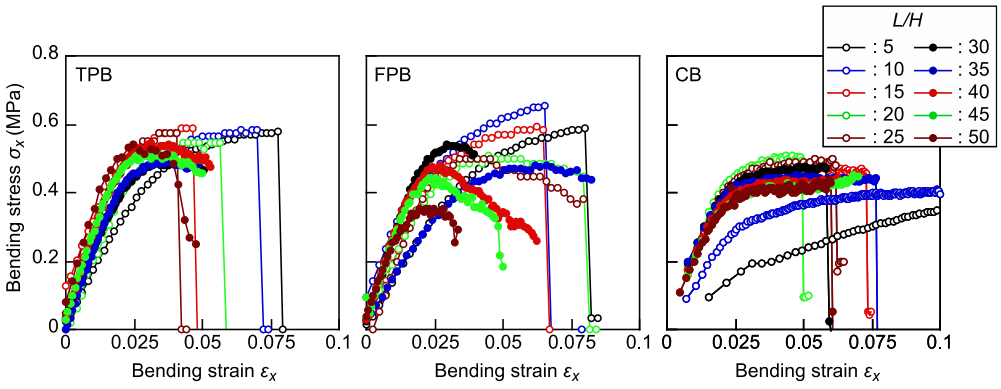

Figure 3. σ_x-ε_x relationships obtained by varying the L/H values in the TPB, FPB, and CB tests.

 doi:10.20944/preprints202405.1113.v1

In the standards for bending tests of CFRP (ASTM D790-17 [28] and ASTM D6272-17 [30]), the methods determined in these standards are not applicable when ε_x exceeds 0.05, and other mechanical properties, such as tensile strength, may be more relevant for characterizing different materials. The results shown in Figure 3 indicate that ε_x at the maximum σ_x often exceeds 0.05 in TPB and FPB tests on samples with L/H values lower than 25. In the standards for the bending tests of cellular solid plastics (ISO 1209-2:2004 [19] and JIS K 7221-2:2006 [20]), the L/H value is determined to be 12-16. However, to determine the bending strength of XPS under $\varepsilon_x < 0.05$, the L/H value should be greater than 16. In contrast, in the CB test, a plateau portion in the σ_x-ε_x relationship was found within the 0.05 ε_x limit when using the samples with L/H values higher than 15.

The results shown in Figure 4 demonstrate the dependence of E_x on L/H in the TPB, FPB, and CB tests. As described above, in the TPB and FPB tests, E_x usually decreases the deflection induced by the shearing force, which is enhanced as the L/H value decreases. The low values of E_x at $L/H = 5$ in the TPB and FPB tests were due to the effect of deflection by the shearing force. However, although the results of previous studies on TPB tests performed using solid wood [33,34] indicate that the dependence of E_x on L/H decreases as the L/H value increases, the E_x values continuously increase in the L/H ranges of 5-50 and 5-40 in the TPB and FPB tests, respectively. In these tests, a slight slippage was induced between the sample and support even when the load was not sufficiently large. Therefore, owing to this slippage, the sample deformed as if it were supported by spans with a distance larger than the actual one. The degree of slippage increased as the L/H value increased; therefore, it can be concluded that the E_x value increases as the L/H value increases. In the CB test, the E_x values at $L/H = 5$ and 10 were lower than those at $L/H \geq 15$. When the L/H value is low, material nonlinearity is induced, and the stiffness of the sample is usually reduced due to the occurrence of material nonlinearity. In contrast, when the CB test is performed using a sample with an L/H value higher than 15, the dependence of E_x on L/H is effectively reduced. Therefore, when a sample with an L/H value lower than 10 was not used, it was more advantageous to use the CB test than the TPB and FPB tests because E_x can be obtained stably without slippage between the sample and span. However, the E_x values obtained from the CB tests are often lower than those obtained from the TPB and FPB tests. Further research is therefore required in order to elucidate the reasons for these differences.

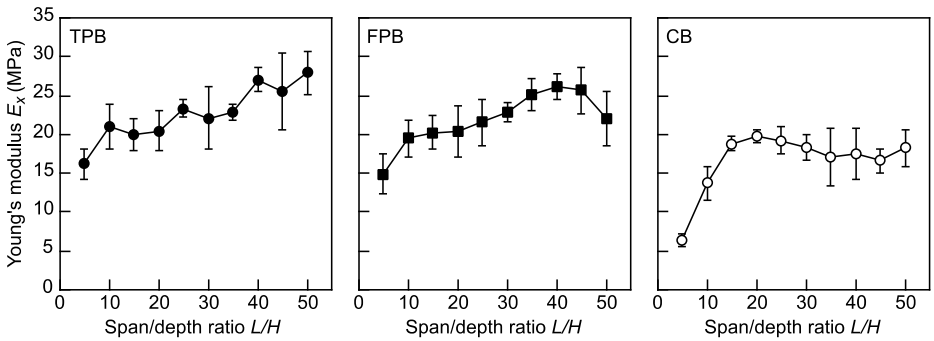

Figure 4. Dependence of E_x on L/H in the TPB, FPB, and CB tests. Data = average ± standard deviations.

Figure 5 shows the dependence of Y_x on L/H in the TPB, FPB, and CB tests. Our statistical analyses revealed no significant differences in the results obtained from the TPB tests. In contrast, significant differences were frequently observed in the results obtained from the FPB and CB tests. The details of the results obtained from the statistical analyses are demonstrated below.

Preprints.org (www.preprints.org) | NOT PEER-REVIEWED | Posted: 17 May 2024 doi:10.20944/preprints202405.1113.v1

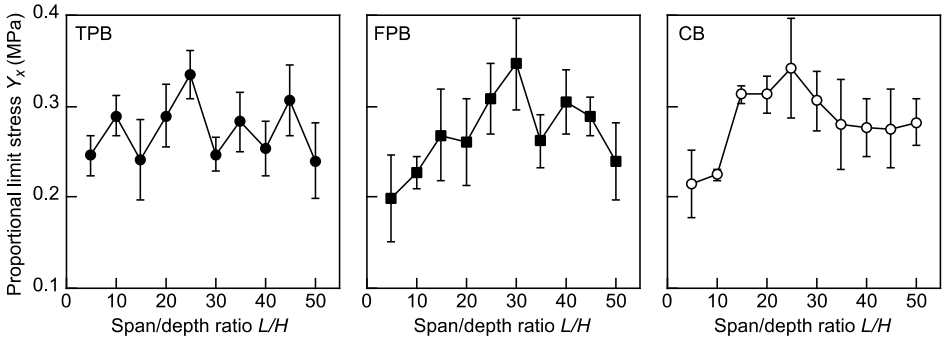

Figure 5. Dependence of Y_x on L/H in the TPB, FPB, and CB tests. Data = average ± standard deviations.

Figure 6 shows the dependence of F_x on L/H in the TPB, FPB, and CB tests. In the TPB test, when F_x is calculated based on EBT, it decreases as the L/H value increases. However, when F_x is calculated using the equations standardized in ASTM D790-17 [28] and JIS K 7074-1988 [29], the dependence of F_x on L/H is effectively reduced. No dependence was observed in the results obtained from the CB tests. In contrast, in the FPB test, the dependence was found to be significant, and the equations determined in ASTM D6272-17 [30] and JIS K 7074-1988 [29] were not effective in reducing the dependence.

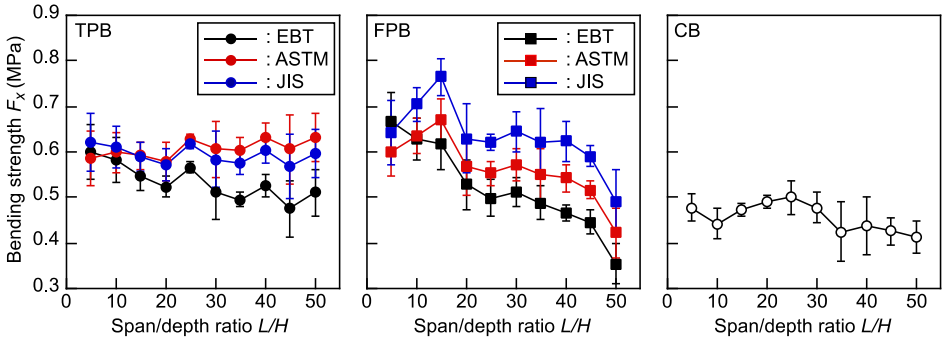

Figure 6. Dependence of F_x on L/H ratio in the TPB, FPB, and CB tests. Data = average ± standard deviations. EBT = elementary beam theory, ASTM = ASTM D790-17 and ASTM D6272-17 in the TPB and FPB tests, respectively, and JIS = JIS K 7074-1988.

In the following section, we discuss the results of our statistical analyses of the samples' bending properties, and the validity of the TPB, FPB, and CB tests.

4. Discussion

The aforementioned results were analyzed via ANOVA (Tukey's tests), and the effects of L/H and the test methods used are discussed below from a statistical perspective.

Table 2 lists the results of the ANOVA for E_x corresponding to L/H. In the TPB and FPB tests, the differences among the averages of E_x were not found in the L/H value range of 25 to 50. In contrast, when $5 \leq L/H \leq 20$, the E_x values were lower than those in the range of L/H values higher than 25 because the deflection due to the shearing force cannot be ignored. Although the L/H was determined to be 15 for the TPB test in ISO 1209-2:2004 [19] and JIS K 7221-2:2006 [20], the results of the statistical analyses suggest that it is preferable to perform TPB tests under L/H values higher than the standardized value. In contrast, in the CB test, differences among the averages of E_x were not found in the L/H value range of 15 to 50, which is wider than the range found in the TPB and FPB tests. Therefore, when considering the range of L/H alone, the CB test is superior to the TPB and FPB tests.

Table 2. ANOVA (Tukey's tests) results for E_x corresponding to L/H.

L/H	5	10	15	20	25	30	35	40	45	50

 doi:10.20944/preprints202405.1113.v1

TPB	A	AB	AC	ACD	BCDE	BCDE	BCDE	E	BDE	**E**
FPB	A	AB	ABC	B	B**D**	B**D**	C**D**	**D**	C**D**	C**D**
CB		A	**B**	**B**	**B**	**B**	A**B**	A**B**	**B**	**B**

The significance level is higher than 0.05 among the samples with the same letters in the horizontal column. The same bold letters in the horizontal column represent the widest range of L/H where the significance level exceeds 0.05.

Table 3 lists the results of the ANOVA for Y_x corresponding to L/H. As described above, there were no significant differences between the Y_x values obtained from the TPB tests. In contrast, in the FPB and CB tests, the L/H range where the differences are not significant is restricted to $20 \leq L/H \leq 50$ and $15 \leq L/H \leq 50$, respectively.

Table 3. ANOVA (Tukey's tests) results for Y_x corresponding to the different L/H.

L/H	**5**	**10**	**15**	**20**	**25**	**30**	**35**	**40**	**45**	**50**
TPB	**A**	**A**	**A**	**A**	**A**	**A**	**A**	**A**	**A**	**A**
FPB	A	AB	AC	A**D**	BC**D**	C**D**	AC**D**	BC**D**	AC**D**	A**D**
CB	A	AB	**C**	**C**	**C**	B**C**	A**C**	AB**C**	AB**C**	AB**C**

The significance level is higher than 0.05 among the samples with the same letters in the horizontal column. The same bold letters in the horizontal column represent the widest range of L/H where the significance level exceeds 0.05.

Table 4 lists the results of the ANOVA for F_x corresponding to L/H. In the TPB tests, the range of L/H values where the differences among the averages are not significant is restricted to $15 \leq L/H \leq 50$ when using the equations based on EBT, but the significant differences are reduced when F_x is calculated using the equations determined in ASTM D 790-17 [28] and JIS K 7074-1988 [29]. In contrast, the differences cannot be reduced sufficiently in the FPB tests, even when ASTM- and JIS-standardized equations are used. In the CB test, no significant differences were observed between the average F_x. The results of the statistical analyses show that the TPB and CB tests are more advantageous than the FPB test.

Table 4. ANOVA (Tukey's tests) results for F_x corresponding to the different L/H.

L/H	**5**	**10**	**15**	**20**	**25**	**30**	**35**	**40**	**45**	**50**
TPB, EBT	A	AB	AB**C**	AB**C**	AB**C**	B**C**	B**C**	AB**C**	**C**	AB**C**
TPB, ASTM	**A**	**A**	**A**	**A**	**A**	**A**	**A**	**A**	**A**	**A**
TPB, JIS	**A**	**A**	**A**	**A**	**A**	**A**	**A**	**A**	**A**	**A**
FPB EBT	A	A	AB	B**C**	**C**	**C**	**C**	**C**	C**D**	D
FPB, ASTM	A	AB	A	A**C**	A**C**	A**C**	B**C**	B**C**	C**D**	D
FPB, JIS	A	AB	A	A**C**	A**C**	A**C**	B**C**	B**C**	C**D**	**C**
CB	**A**	**A**	**A**	**A**	**A**	**A**	**A**	**A**	**A**	**A**

The significance level is higher than 0.05 among the samples with the same letters in the horizontal column. The same bold letters in the horizontal column represent the widest range of L/H where the significance level exceeds 0.05. EBT = elementary beam theory, ASTM = ASTM D790-17 and ASTM D6272-17 in the TPB and FPB tests, respectively, and JIS = JIS K 7074-1988.

Table 5 lists the E_x, Y_x, and F_x values obtained by averaging those in the L/H range, where the significance level is higher than 0.05. The E_x, Y_x, and F_x values obtained from the TPB and FPB tests were similar. In contrast, the E_x and F_x values obtained from the CB tests were lower than those obtained from the TPB and FPB tests, whereas the Y_x values obtained from the CB tests were close to those obtained from the TPB and FPB tests. These tendencies are often discrepant from those obtained using CFRP [21–23], solid wood [24], plywood and MDF [25,26], and cardboard [27]. Further research is thus required to elucidate the discrepancies between the results obtained using different materials.

 doi:10.20944/preprints202405.1113.v1

Table 5. E_x, Y_x, and F_x in the L/H range, where the significance level exceeded 0.05.

Method	E_x (MPa)	Y_x (MPa)	F_x EBT (MPa)	F_x ASTM (MPa)	F_x JIS (MPa)
TPB	24.8 ± 3.5	0.273 ± 0.049	0.520 ± 0.045	0.606 ± 0.047	0.593 ± 0.046
FPB	23.9 ± 3.0	0.287 ± 0.049	0.490 ± 0.043	0.551 ± 0.042	0.602 ± 0.070
CB	18.1 ± 2.5	0.298 ± 0.040	0.457 ± 0.046	-	-

Data = average ± standard deviations. EBT = elementary beam theory, ASTM = ASTM D790-17 and ASTM D6272-17 in the TPB and FPB tests, respectively, and JIS = JIS K 7074-1988.

5. Conclusions

In this study, three-point bending (TPB), four-point bending (FPB), and compression bending (CB) tests were performed on extruded polystyrene (XPS) samples to determine their bending properties. The dependence of the properties on the span/depth ratio was statistically analyzed (Tukey's tests), and the applicability of the three test methods was examined. Through our analyses, the following results were obtained:

(1) In the TPB and FPB tests, Young's modulus increased continuously as the span/depth ratio increased because of the slippage between the sample and supporting point, as well as the effect of deflection caused by the shearing force. In the CB test, the Young's modulus was lower in the small span/depth ratio range where material nonlinearity was induced by axial loading prior to bending deformation. Except for this span/depth ratio range, Young's modulus could be obtained while reducing the effect of the sample configuration.

(2) The effect of the span/depth ratio on the proportional limit stress was not observed in the TPB test results; in contrast, the effect was found in the results obtained from the FPB and CB tests.

(3) To determine the samples' bending strength by using the TPB test, the methods for correcting the large defection determined in ASTM D 790-17 and JIS K 7074-1988 were effective; the correction methods for the FPB test determined in ASTM 6272-17 and JIS K 7074-1988 were not sufficient, however. In contrast, the effect of the span/depth ratio was not significant in the CB test results.

(4) From the experimental results, the use of TPB and CB tests is recommended over the FPB test to determine the bending properties of XPS samples. However, the properties determined via the TPB and CB tests were different. Further research should be therefore conducted to explore the source of these differences in more detail.

6. Nomenclature

B = sample width
H = sample depth
E_x = Young's modulus in the length direction of the sample
F_x = bending strength in the length direction of the sample
L = length between the spans
P = load applied to the sample
P_{max} = maximum load
x = displacement at the loading point in the compression bending test
$\dot{x}$ = crosshead speed
Y_x = proportional limit stress in the length direction of the sample
δ_L = deflection at the loading point in the four-point bending test
δ_M = deflection at the midspan
δ_{Mb} = deflection at the midspan at $P = P_{max}$
ε_x = bending strain at the midspan
$\dot{\varepsilon}_x$ = strain rate at the midspan
κ_M = curvature at the midspan
σ_x = bending stress at the midspan
ANOVA = analysis of variance
CB = compression bending

 doi:10.20944/preprints202405.1113.v1

EBT = elementary beam theory
FPB = four-point bending
TPB = three-point bending
L, T, and Z = length, width, and thickness directions of the panel, respectively
XPS = extruded polystyrene

Author Contributions: Conceptualization, H.Y.; methodology, H.Y.; software, H.Y.; validation, H.Y., M.Y. and M.M.; formal analysis, H.Y.; investigation, H.Y.; resources, H.Y.; data curation, H.Y. and M.W.; writing—original draft preparation, H.Y.; writing—review and editing, H.Y.; visualization, H.Y.; supervision, M.Y. and M.M.; project administration, H.Y. All the authors have read and agreed to the published version of the manuscript.

Funding: This research received no external funding.

Acknowledgments: This work was supported by JSPS KAKENHI Grant Number 23K26970.

Conflicts of Interest: The authors declare no conflicts of interest.

References

1. Kim, J.; You, Y.-C. Composite behavior of a novel insulated concrete sandwich wall panel reinforced with GFRP shear grids: effect of insulation types. *Materials* **2015**, *8*, 899-913.
2. Cai, S.; Zhang, B.; Cremaschi, L. Review of moisture behavior and thermal performance of polystyrene insulation in building applications. *Build. Environ.* **2017**, *123*, 50-65.
3. Li, Q.; Wei, H.; Han, L.; Wang, F.; Zhang, Y.; Han, S. Feasibility of using modified silty clay and extruded polystyrene (XPS) board as the subgrade thermal insulation layer in a seasonally frozen region, Northeast China. *Sustainability* **2019**, *11*, 804.
4. Aksit, M.; Zhao, C.; Klose, B.; Kreger, K.; Schmidt, H.-W.; Altstädt, V. Extruded polystyrene foams with enhanced insulation and mechanical properties by a benzene-trisamide-based additive. *Polymers* **2019**, *11*, 268.
5. Li, Q.; Wei, H.; Zhou, P.; Zhang, Y.; Han, L.; Han, S. Experimental and numerical research on utilizing modified silty clay and extruded polystyrene (XPS) board as the subgrade thermal insulation layer in a seasonally frozen region, Northeast China. *Sustainability* **2019**, *11*, 3495.
6. Seto, H.; Saito, I.; Onuki, A.; Takeuchi, M.; Tsuchiya, T. Presumption of the source of indoor air pollution. Amounts of styrene and butanol generation from construction materials. *Ann. Rep. Tokyo Metr. Res. Lab. P. H.* **2000**, 51, 219-222.
7. Aoyagi, R.; Matsunobu, K.; Matsumura T. Development of continuous vapor generation for calibration styrene with permeation tube method. *Indoor Environ.* **2009**, 52, 97-102.
8. Matsumoto, T.; Iwamae, A.; Wakana, S.; Mihara, N. Effect of the temperature-humidity condition in the room and under the floor by heat insulation tatami and flooring. Summaries of Technical Papers of Annual Meeting, Kobe, Japan, 13 September; Architectural Institute of Japan (Environmental Engineering II): Tokyo, Japan, 2014.
9. Vinson, J.R. Sandwich structures. *Appl. Mech. Rev.* **2001**, 54, 201-214.
10. Hu, Y.; Nakao, T.; Nakai, T.; Gu, J.; Wang, F. Dynamic properties of three types of wood-based composites. *J. Wood Sci.* **2005**, 51, 7-12.
11. Hu, Y.; Nakao, T.; Nakai, T.; Gu, J.; Wang, F. Vibrational properties of wood plastic plywood. *J. Wood Sci.* **2005**, 51, 13-17.
12. Kawasaki, T.; Kawai, S. Thermal insulation properties of wood-based sandwich panel for use as structural insulated walls and floors. *J. Wood Sci.* **2005**, 52, 75-83.
13. Kilar, V.; Koren, D.; Bokan-Bosiljkov, V. Evaluation of the performance of extruded polystyrene boards – implications for their application in earthquake engineering. *Polym. Test*. **2014**, *40*, 234-244.
14. Vitau, C.; Dudescu, M.C. Investigation of mechanical behaviour of expanded polystyrene under compressive and bending loadings. *Mater. Plast.* **2020**, *57*, 199-207.
15. Tang, N.; Lei, D.; Huang, D.; Xiao, R. Mechanical performance of polystyrene foam (EPS): experimental and numerical analysis. *Polym. Test.* **2019**, *73*, 359-365.
16. Yoshihara, H.; Ataka, N.; Maruta, M. Measurement of the Young's modulus and shear modulus of extruded polystyrene foam by the longitudinal and flexural vibration methods. *J. Cell. Plast.* **2018**, *54*, 199-216.
17. Yoshihara, H.; Wakahara, M.; Yoshinobu, M.; Maruta, M. Torsional vibration tests of extruded polystyrene with improved accuracy in determining the shear modulus. *Polymers* **2022**, *14*, 1148.
18. Yoshihara, H.; Maruta, M. Measurement of the shear properties of extruded polystyrene by in-plane shear and asymmetric four-point bending tsts. *Polymers* **2020**, *12*, 4

 doi:10.20944/preprints202405.1113.v1

19. ISO 1209-02-2004, Rigid cellular plastics—Determination of flexural properties—Part 2 : Determination of flexural strength and apparent flexural modulus of elasticity, International Organization for Standardization, Geneva, Switzerland, 2004
20. JIS K 7221-2:2006, Rigid cellular plastics-Determination of flexural properties-Part 2 : Determination of flexural strength and apparent flexural modulus of elasticity, Japan Standards Association, Tokyo, Japan, 2006
21. Fukuda, H. A new bending test method of advanced composites. Exp. Mech. **1989**, *29*, 330-335.
22. Fukuda, H.; Katoh, H.; Uesugi, H. A modified procedure to measure bending strength and modulus of advanced composites by means of compression bending. J. Compos. Mater. **1995**, *29*, 195-207.
23. Fukuda, H.; Itabashi, M. Simplified compression bending method for advanced composites. Compos. A **1999**, *30*, 249-256.
24. Yoshihara, H.; Oka, S. Measurement of bending properties of wood by compression bending tests. *J. Wood Sci.* **2001**, *47*, 262-268.
25. Yoshihara, H. Bending properties of medium-density fiberboard and plywood obtained by compression bending test. *Forest Prod. J.* **2010**, *61(1)*, 56-63.
26. Santabárbara, A. G., Carrió, J. M., Sastre, R. S., Sakata, H. Determination of bending properties of lauan plywood by compression bending tests. In Proceedings, 6th Int. Confer. Technol. Innov. Build. (CITE 2021), Madrid, Spain, (25 3 2021).
27. Yoshihara, H.; Yoshinobu, M.; Maruta, M. Bending stiffness and moment capacity of cardboard obtained from three-point and elastica bending tests. *Nord. Pulp Paper Res. J.* **2023**, *38*, 73-85.
28. ASTM D790-17, Standard test methods for flexural properties of unreinforced and reinforced plastics and electrical insulating materials, ASTM International, West Conshohocken, PA, 2017
29. JIS K 7074-2:1988, Testing methods for flexural properties of carbon fiber reinforced plastics, Japan Standards Association, Tokyo, Japan, 1988
30. ASTM D6272-17, Standard test methods for flexural properties of unreinforced and reinforced plastics and electrical insulating materials by four-point bending, ASTM International, West Conshohocken, PA, 2017
31. Adams, D. F.; Carlsson, L. A.; Pipes, R. B. Lamina flexural response. In *Experimental characterization of advanced composite materials. 3rd Ed.*; CRC Press: Boca Raton: USA; 2003, pp. 121-130.
32. Davies, P.; Blackman, B. R. K.; Brunner, A. J. Mode II delamination. In *Fracture mechanics testing methods for polymers adhesives and composites.* Moore, D. R.; Pavan, A.; Williams, J. G., Eds.; Elsevier: Amsterdam: Netherland; 2001; ESIS Publication 28, pp. 307-333.
33. Yoshihara, H.; Kubojima, Y.; Ishimoto, T. Several examinations on the static bending test methods of wood by using todomatsu (Japanese fir). *Forest Prod. J.* **2003**, *53(2)*, 39-44.
34. Yoshihara, H.; Itoh, A. Influence of large deflection on the measurement of bending properties of veneer by three-point static bending tests. *Wood Fiber Sci.* **2003**, *35*, 293-300.